Effect of high intensity ultrasound on the mesostructure of hydrated zirconia

2012 J. Phys.: Conf. Ser. 340 012057

(http://iopscience.iop.org/1742-6596/340/1/012057)

Effect of high intensity ultrasound on the mesostructure of hydrated zirconia

G.P. Kopitsa[1*], A.E. Baranchikov[2], O.S. Ivanova[2], A.D. Yapryntsev[3], S.V. Grigoriev[1], P. Klaus Pranzas[4], V.K. Ivanov[2]

[1]Petersburg Nuclear Physics Institute, Gatchina 188300, Russia
[2]Institute of General and Inorganic Chemistry, Moscow 119991, Russia
[3]Moscow State University, Department of Materials Science, Moscow 119991, Russia
[4]GKSS Research Centre, Geesthacht, 21502, Germany
E-mail: kopitsa@lns.pnpi.spb.ru

Abstract. We report structural changes in amorphous hydrated zirconia caused by high intensity ultrasonic treatment studied by means of small-angle neutron scattering (SANS) and X-ray diffraction (XRD). It was established that sonication affects the mesostructure of $ZrO_2 \times xH_2O$ gels (i.e. decreases their homogeneity, increases surface fractal dimension and the size of monomer particles). Ultrasound induced structural changes in hydrated zirconia governs its thermal behaviour, namely decreases the rate of tetragonal to monoclinic zirconia phase transition.

1. Introduction

Recently considerable progress was achieved in the field of application of high intensity ultrasonic treatment to nanomaterials synthesis. In the last few years a number of papers and reviews devoted to the development of advanced sonochemical methods of nanopowders and nanocomposites preparation were published [1].

Specific physical and chemical effects taking place during sonication of liquids arise mostly from acoustic cavitation, i.e. formation of vapour-gas microbubbles and their further oscillations and collapse. The mechanism of sonochemical processes in homogeneous liquids is well studied and thus obtained data are usually treated in the frames of two major theories, namely, hot spot theory [2] and the theory of local electrization [3]. The former supposes that high local temperatures (up to several thousand degrees) and pressures (several kilobars) arise during the collapse of cavitation bubbles. The latter explains the mechanism of sonochemical reactions through high local electric potentials formed on the surface of microcavities leading to intensive electrical discharges. In both cases extreme conditions in the cavities lead to decomposition of volatile compounds dissolved in the liquid (for instance, organometallic compounds, metal complexes etc.) and formation of nanostructured products.

On the contrary, information on the specific action of high intensity ultrasound on heterogeneous liquid-solid systems is still rather poor. It is generally accepted that the collapse of cavitation bubbles in the vicinity of the phase boundary (e.g. solid-liquid interface) occurs asymmetrically and subject it to shockwaves and local microjets of liquid. Thus, acoustic treatment of suspensions consisting of relatively large crystalline particles, which size is comparable to the size of a collapsing cavitation

* Author to whom correspondence should be addressed

bubble (d > 0.5–1 μm) leads to several specific effects including de-agglomeration, decrease of mean particle size, increase of the surface area due to erosion, etc. [1]. In turn, investigations concerning the influence of sonication on heterogeneous systems (for instance, sols and gels) consisting of substantially smaller particles were performed on a quite limited number of systems, mostly silica xerogels [4]. It was established that ultrasonication leads to the increase of the rate of gel formation and changes the mesostructure (e.g. density, size of monomers and size of aggregates) of gels. Nevertheless the effects of ultrasonication on such systems are to be further ascertained. For instance, recently we have established that ultrasonication affects the fractal structure of amorphous iron(III) oxide and governs its crystallization behaviour under hydrothermal conditions [5].

In view of this circumstance the present work aims to analyze the influence of high intensity ultrasound on the mesostructure and fractal structure of amorphous hydrated zirconia xerogels. Our investigation was primarily based on the use of small-angle neutron scattering method (SANS) which is widely used in the study of nuclear and magnetic inhomogeneities in various amorphous materials [6]. Structural changes in ZrO_2 caused by ultrasonication were also corroborated by means of X-ray diffraction (XRD) and low-temperature nitrogen adsorption. This paper continues the series of our research reports connected with studies of mesostructure and fractal properties of amorphous hydrated oxides. Experimental results reported in this paper not only comply with our previous findings on the ultrasonic-assisted synthesis of oxide materials, but also significantly expand our understanding of the principles of evolution of amorphous hydrated oxides in course of crystallization.

2. Experimental

2.1. Synthesis of samples

Hydrated zirconia gels were precipitated from zirconium oxynitrate (99%, Aldrich) solutions as follows: 50 ml of zirconium oxynitrate aqueous solution (C_0 = 0.10, 0.25 or 1.00 mole·L^{-1}) were added dropwise to 50 ml of ammonia aqueous solution (7.5 mole·L^{-1}) under vigorous stirring. The total duration of the precipitation procedure was 15 min. Gels of hydrated zirconia were also precipitated under the same conditions but under ultrasonic treatment performed using Bandelin Sonopuls HD 3200 generator operated at 20 kHz and equipped with titanium horn (TT-13 titanium tip). The output power measured using standard calorimetric technique was 59 W·cm^{-2}. During precipitation procedure ultrasonic horn was immersed 10 mm below the surface of the treated media. To prevent uncontrollable rise of the temperature due to dissipation of acoustic energy the precipitation process was conducted in the thermostated cell (25°C).

Upon completion of the sedimentation procedure the suspensions were additionally stirred for 30 min with (for sonicated samples) or without (for control ones) ultrasonic treatment. As synthesized hydrated zirconia gels were centrifuged (8000 min^{-1}) and washed several times with distilled water until the conductivity of mother liquor as measured using Hanna HI 98312 conductometer was less than 0.3 mS. Gels were further dried in air at 60°C overnight to produce hydrated zirconia xerogels. Throughout the paper hydrated zirconia xerogels synthesized from 0.10, 0.25 and 1.00 mole·L^{-1} solutions under ultrasonic treatment (US) and without sonication (C) are named Z-1US, Z-2US, Z-3US, Z-1C, Z-2C and Z-3C, respectively.

Thermal decomposition of the xerogels was conducted in a muffle furnace in air at 500 and 600 °C for 5 h. Heating rate was 10 °C/min. After the annealing samples were cooled down to ambient temperature within the furnace. Resulting zirconia powders are named hereafter X–T (here, X is a designation of the initial xerogel, and T is the temperature of treatment – 500 or 600 °C).

2.2. Methods of analysis

SANS measurements were performed on SANS-2 setup (FRG-1 neutron reactor, GKSS Research Centre, Geesthacht, Germany). The experiments were performed at neutron wavelength λ = 0.58 nm with $\Delta\lambda/\lambda$ = 10% and for four sample-detector distances *SD* = 1, 3, 7 and 20.7 m, which allowed to

perform the measurements of the neutron scattering intensity for momentum transfers in the range $2.6 \cdot 10^{-2} < q < 2.6$ nm^{-1}. The scattered neutrons were detected by a two-dimensional position-sensitive ^3He detector (256×256 cells, *x* slope/ *y* slope – 2.2mm/ 2.2mm).

Samples of the xerogels were placed in a 1 mm thick quartz cells. Apparent density ρ_H of each sample was calculated as a weight of a powder divided by its volume. The initial spectra for each q range were corrected using the standard procedure [7] taking into account the scattering from the setup equipment and cell, as well as background from incoherent scattering of neutrons on hydrogen atoms which are present in samples in the form of physically and chemically bounded water. Resulting 2D isotropic spectra were averaged azimuthally and their absolute values were determined by normalizing to the incoherent scattering cross section from vanadium with inclusion of the detector efficiency and apparent density (ρ_H) for each sample. All measurements were done at room temperature.

The SANS intensity analyzed hereafter was defined as

$$I_s(q) = I(q) - T \cdot I_0(q) \tag{1}$$

where $I(q)$ and $I_0(q)$ are the momentum-transfer distributions of scattered neutrons behind the sample and beam without the sample, respectively; and T is the reduction of the transmitted beam, *i.e.*, the transmission coefficient.

The measured value of the SANS intensity, $I_s(q)$, is related to the scattering law $S(q)$ through the following expression:

$$I_s(q) = I \cdot L \cdot \int F(q - q_1) S(q) dq_1 \tag{2}$$

where L is the sample thickness and $F(q)$ – setup resolution function, which was approximated by a Gaussian and was calculated separately for each *SD* distance with the use of the standard procedure [8].

In addition to SANS, information on the structure of gels was obtained from the value of transmission coefficient $T = I(0)/I_0$. It is known [9] that intensities $I(0)$ and I_0 are related as

$$I(0) = I_0 \cdot \exp(-\Sigma_{tot} \cdot L) \tag{3}$$

where $\Sigma_{tot} = \sigma_s + \sigma_a$ is the integral scattering cross section which includes nuclear scattering σ_s and absorption σ_a.

Thermogravimetric and differential thermal analyses (TGA/DTA) of the xerogels were performed in air using Pyris Diamond thermoanalyzer (Perkin-Elmer) in the temperature range 20–800 °C (heating rate 10 °C/min).

X-ray powder diffraction (XRD) patterns were obtained using Rigaku D/MAX 2500 diffractometer (CuK_α radiation) over a 2θ range of 10–85 ° with an increment 0.02 °/step at the rate 2 °/min. Particle size was estimated using Scherrer equation

$$D = \frac{K\lambda}{[\beta(2\theta) - s]\cos\theta_0} \tag{4}$$

Here, θ_0 is the peak position, λ is the radiation wavelength, $\beta(2\theta)$ – FWHM of a corresponding peak, s – instrumental broadening (is equal to 0.1 ± 0.01 °2θ). The value of K (shape factor) was set equal to 1. The $\beta(2\theta)$ values were determined by subtraction of background followed by fitting profiles of (111) and $(1\bar{1}1)$ reflections of monoclinic zirconia and (111) reflection of tetragonal zirconia to the Voigt pseudo-functions.

Volume fractions of monoclinic (m-ZrO_2) and tetragonal (t-ZrO_2) phases in zirconia samples were estimated using equations proposed by Toraya et al. [10].

Specific surface area (S_{BET}) of samples was measured by low temperature nitrogen adsorption conducted using ATX-6 analyzer (Katakon, Russia). Before measurements the samples were outgased

at 200 °C for 30 min under dry helium flow. Calculation of specific surface area was carried out within 8-point Brunauer-Emmett-Teller (BET) method.

3. Results and discussion

X-ray diffraction analysis has confirmed that all the initial xerogels are of amorphous nature giving two extremely broad diffraction peaks at ~30 and ~50–60 °2θ (see figure 1). Such X-ray patterns are quite common for as precipitated hydrous zirconia and according to [11] arise from short-range ordering in zirconium hydroxide polymers.

Thermal analysis of the xerogels has shown that their decomposition occurs in an identical way. Namely, overall weight loss is equal to 77–80 mass.% regardless of application of ultrasound during precipitation process and regardless of concentration of zirconium oxynitrate in the starting solutions. Typical thermal analysis data are presented in figure 1.

Here, weight loss at temperatures up to approximately 400 °C corresponds to elimination of physisorbed and chemically bounded water, which is accompanied by broad endothermic effect. Sharp exothermic peak at ~450 °C is obviously due to formation of nanocrystalline zirconia. These data are in line with our previous results. It has been shown [12] that hydrated zirconia synthesized in acidic media (when pH is lower than the point of zero charge) contains high amount of adsorbed NO_3^- ions. Thermal treatment of resulting xerogels is accompanied not only by elimination of physically and chemically bounded water, but also by a significant weight loss at $t > 400$ °C caused by decomposition of nitrates. On the other hand, hydrated zirconia precipitated under alkaline conditions, as it was done in this work, contains only trace amount of such impurities.

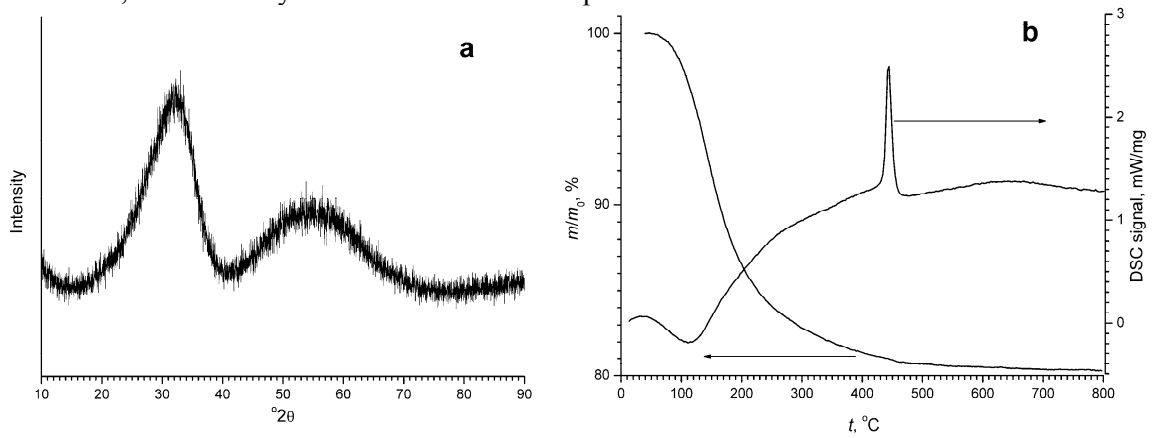

Figure 1. XRD (a) and TGA and DTA (b) data for Z-2US hydrated zirconia xerogel.

Thus basing on TGA data we can conclude that chemical composition of all the xerogels can be approximately ascribed as $ZrO_2 \cdot 1.7H_2O$ and it is almost identical regardless of synthetic procedure. This fact gives us an additional basis for the validity of SANS data comparison.

Figure 2 shows the experimental curves of differential neutron cross section $d\Sigma(q)/d\Omega$ *vs.* momentum transfer q for amorphous zirconia xerogels precipitated under various conditions. Comparison of these spectra gives an evidence that in all the cases increase in the concentration of starting zirconium oxynitrate solution results in an increase in the SANS intensity, indicating a decrease in the nuclear density homogeneity of corresponding xerogels in the range of 1–100 nm. One can also see that in the case of control samples dependence of SANS intensity upon the concentration of starting solution is much more pronounced than in case of ultrasonicated gels.

This effect is even more pronounced when the integral SANS cross-sections are compared (figure 3). Integral cross sections for the samples prepared from concentrated solutions (0.25 and 1.00 mole·L^{-1}) with or without ultrasonication are nearly identical indicating that the difference in their nuclear homogeneity is negligible. On the other hand, hydrated zirconia precipitated from diluted

oxynitrate solution (0.10 mole·L^{-1}) under ultrasonic action possesses lower nuclear homogeneity in comparison with the corresponding control sample.

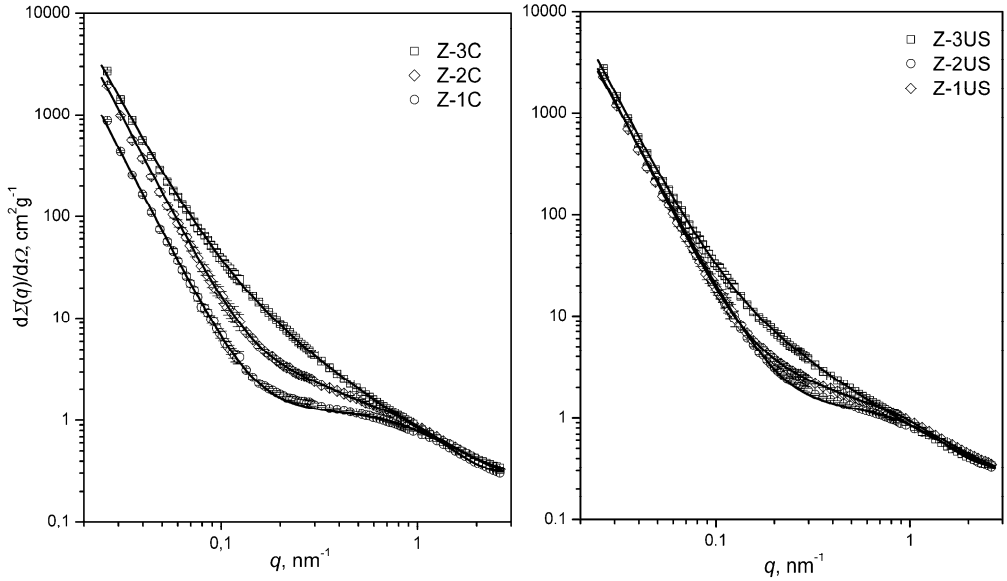

Figure 2. SANS differential cross-sections $d\Sigma(q)/d\Omega$ for amorphous $ZrO_2 \cdot xH_2O$ xerogels *vs*. momentum transfer q. Designations of corresponding samples are given in the pictures. Fitting of experimental data with formula (6 and 9) is given with firm lines.

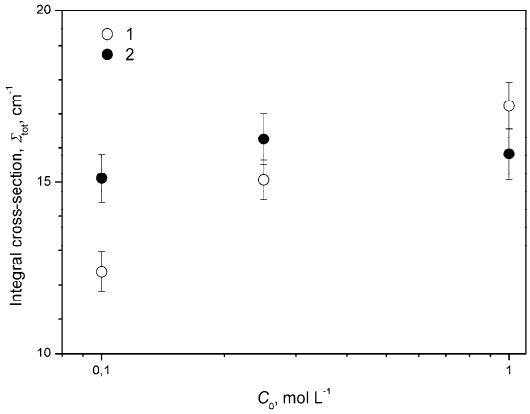

Figure 3. Integral SANS cross-sections Σ_{tot} for amorphous $ZrO_2 \cdot xH_2O$ xerogels *vs*. concentration of starting zirconium oxynitrate solution (1 – control samples; 2 – sonicated ones).

Figure 3 also demonstrates that in the control series of the gels increase in the concentration of starting solutions results in notable decrease in nuclear homogeneity. Application of ultrasound diminishes this effect so that nuclear homogeneity of samples synthesized from different starting solutions is practically identical.

In SANS experiments, the power-law momentum-transfer dependence of the scattering intensity is usually observed in the form $I(q) \sim q^{-n}$ ($n \leq 6$) in a certain momentum-transfer region $q > 1/R$, where R is the characteristic scale of the scattering system. The fractal dimension of the system and the correlation function of scattering inhomogeneities are determined by the n value or, more precisely, by the deviation from the Porod asymptotic ($n = 4$). For volume and mass fractals, n coincides with the fractal dimension D_V, $1 \leq D_V \leq 3$. For the scattering from three-dimensional objects with fractal surfaces $3 < n = 6 - D_S \leq 4$, where D_S is the surface fractal dimension, $2 \leq D_S \leq 3$.

It should be emphasized that a common property for all the samples under study is that corresponding spectra can be divided into two various q ranges, where the behaviour of the SANS cross section $d\Sigma(q)/d\Omega$ is significantly different (see figure 2). In particular, for low q values ($q < q_c$, where $q_c \approx 0.15$ nm^{-1} is the transition point between one scattering regime to another) the scattering cross section for all the samples satisfies the power law q^{-n}. As known, such a power-law dependence

is observed for wide size distribution of scattering inhomogeneities with the relation $R_{max} >> R_{min}$ if the condition

$$R_{max}^{-1} << q << R_{min}^{-1}. \quad (5)$$

is satisfied. In addition, the power scattering law means that inhomogeneities making the dominant contribution to scattering are sufficiently large, so that $q_{min}R >> 1$. Bale and Schmidt [13] proposed a more exact applied criterion for a certain characteristic size of inhomogeneities, $q_{min}R \approx 3.5$. In our case, $q_{min} = 2.6 \cdot 10^{-2}$ nm^{-1} and the characteristic size of inhomogeneities is equal to $R \approx 135$ nm.

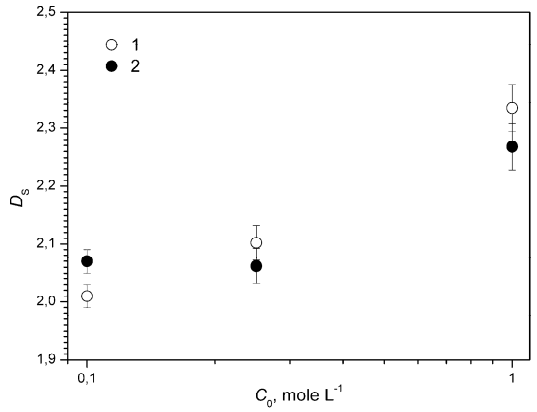

Figure 4. Surface fractal dimension (D_S) of amorphous zirconia xerogels versus concentration of initial solution (1 – control samples; 2 – sonicated ones).

The exponent n values found from the slope of the straight-line parts of the curves plotted in log-log scale (see figure 2) lie in the range from 3.67 to 3.99 (see table 1). This corresponds to the scattering from the fractal surfaces with the dimension $2.01 < D_S = 6 - n < 2.33$ (figure 4).

Thus, the further analysis of scattering in the region $q < q_c$ has been performed using the two-phase model (solid phase–pore) of the porous structure with the fractal surface of the phase interface [14]. According to this model, an object consists of inhomogeneities possessing strongly developed surface, so that, if the total area of the inhomogeneity surface measured in the scale of the inhomogeneity surface size R is proportional to R^2, the area of the surface of the scale $r << R$ is equal to $R^2(R/r)^{\Delta}$, where $0 < \Delta < 1$ and $n = 4 - \Delta$. In this case, the fractal dimension of the surface, $D_S = 2 + \Delta$, is larger than two.

Table 1. Parameters of mesostructure of amorphous hydrated zirconia samples according to SANS measurements.

Sample designation	Z-1C	Z-1US	Z-2C	Z-2US	Z-3C	Z-3US
ρ_H, g·cm^{-3}	1.485	1.68	1.62	1.794	1.58	1.78
T	0.73 ± 0.01	0.66 ± 0.01	0.67 ± 0.01	0.62 ± 0.01	0.64 ± 0.01	0.63 ± 0.01
Σ_{tot}, cm^{-1}	12.4 ± 0.6	15.1 ± 0.7	15.1 ± 0.6	16.3 ± 0.8	17.2 ± 0.6	15.8 ± 0.6
$A_1 \times 10^3$, cm^{-2}·g^{-1}	1.22 ± 0.07	5.77 ± 0.21	2.42 ± 0.20	5.53 ± 0.33	4.83 ± 0.57	3.57 ± 0.34
$D_S = 6 - n$	2.01 ± 0.02	2.07 ± 0.02	2.10 ± 0.03	2.06 ± 0.03	2.33 ± 0.04	2.27 ± 0.04
A_2, cm^2·g^{-1}	0.95 ± 0.01	1.02 ± 0.01	3.20 ± 0.08	1.91 ± 0.11	–	–
r_g, nm	1.41 ± 0.03	1.42 ± 0.03	4.62 ± 0.05	4.68 ± 0.04	–	–
$D_V = m$	–	–	–	–	1.80 ± 0.05	1.45 ± 0.05

Deviation from the power law q^{-n} is observed for all the samples (sonicated and non-sonicated) at higher values of momentum transfer. For the samples prepared from 0.10 and 0.25 mole·L^{-1} zirconium oxynitrate solutions (with or without ultrasonication), in the region $q > q_c$, the scattering curves exhibit a so-called "shoulder" indicating the presence of small inhomogeneities with characteristic size r_c. In this region the function $d\Sigma(q)/d\Omega$ exhibits Guinier behaviour. Thus, the observed scattering pattern indicates that the Z-1US, Z-2US, Z-1C and Z-2C xerogels contain two types of scattering inhomogeneities with strongly different characteristic scales which correspond to relatively large aggregates with the strongly developed surface that are formed from the initial small monomer

particles. Analysis of the curve's slopes in Guinier region ($\ln(d\Sigma(q)/d\Omega)$ versus q^2) allows one to evaluate the values of the gyration radii r_g of small inhomogeneities as well as their characteristic size r_c. For instance, characteristic size of spheres can be calculated as $r_c = \sqrt{5/3}\, r_g$ [15]

The power-law dependence of the scattering cross section $d\Sigma(q)/d\Omega$ is usually observed for large q values, whereas the Guinier regime from which an upper estimate can be obtained for the scale of scattering inhomogeneities is observed for small q values. The absence of the Guinier region on the scattering curves for low q values means that the gyration radius R_g or, for the fractal systems, the upper self-similarity boundary is larger than the maximum size R_{max} of the inhomogeneities scattering from which can be detected in the experiment with a given resolution. In turn, the lower self-similarity boundary is likely determined by the size r_c of the small inhomogeneities.

In turn, SANS cross section for Z-3US and Z-3C samples prepared from concentrated solutions with or without ultrasonication, in the region $q > q_c$ obeys q^{-m} law, where the exponent m values are 1.45 and 1.8, respectively. This corresponds to the scattering from the volume fractals with the dimension $D_V = m = 1.45$ and 1.8, respectively [14]. Results obtained indicate that synthesis of xerogels from concentrated solutions lead to formation of volume fractal clusters consisting of primary particles. These clusters, in turn, form large-scale aggregates possessing well-developed fractal surface.

In general, we can conclude that scattering from hydrous zirconia samples under this study is in a good accordance with our previously reported data [12] indicating that scattering on amorphous zirconia xerogels precipitated at pH > 6 can be described within the model of porous structure with fractal surface.

In view of this circumstance, we used the following expression to analyze scattering from Z-1US, Z-2US, Z-1C and Z-2C xerogels over the entire q range [12]:

$$\frac{d\Sigma(q)}{d\Omega} = \frac{A_1(D_S)}{q^n} + A_2 \cdot \exp\left(-\frac{q^2 r_g^2}{3}\right) + I_{inc}\,. \tag{6}$$

Here, $A_1(D_S)$ and A_2 are the free parameters first of which depends on the system fractal dimension [13] and the second is proportional to the product of the number of monodisperse inhomogeneities in the scattering volume and the neutron scattering amplitude density ρ [15]. The parameter I_{inc} is a constant that is independent of q and is associated with incoherent scattering on hydrogen atoms in xerogels.

It is well known that for porous materials consisting of two homogeneous phases A_1 is related to the phase-interface surface as [13]:

$$A_1(D_S) = \pi\rho^2\Gamma(5-D_S)\sin[(D_S-1)(\pi/2)]N_0\,, \tag{7}$$

where N_0 is the characteristic of the fractal boundary, Γ is the gamma function, ρ_h is the solid-phase density, and ρ for a molecule containing several elements is defined as:

$$\rho = \sum_i b_i N_i \frac{\rho_h N_A}{M}\,. \tag{8}$$

Here, N_A is the Avogadro constant, M is the molar mass, b_i is the scattering length for the i-th element in the molecule, and N_i is the number of atoms of this element. The constant N_0 in Eq. (7) is related to the specific surface (S_0) of the surface fractal as $S_0 = N_0 r^{2-Ds}$, where r^{2-Ds} is determined by the length of the yardstick. For smooth surfaces, $D_S = 2$ and $N_0 = S_0$.

Taking into account that for the Z-3C and Z-3US xerogels the crossover from one power-law dependence to another occurs at $q_c \approx 0.15$ nm^{-1}, we used the following expression to analyze scattering from these samples:

$$\frac{d\Sigma(q)}{d\Omega} = \frac{A_1(D_S)}{q^n} + \frac{A_3(D_V)}{q^m} + I_{inc}\,. \tag{9}$$

To obtain the final results, expressions (Eq. (6) and (9)) were convolved with the setup resolution function. The experimental curves of the differential cross section $d\Sigma(q)/d\Omega$ versus q were processed by the least mean squares method over the entire q range under investigation. The results of this analysis are given in figures 2 and 4 and in Table 1.

To analyze quantitatively the influence of ultrasonic treatment on the structure of amorphous xerogels we have compared the scattering from sonicated and non-sonicated samples. The results of such a comparison are presented in figure 5 as a difference in scattering as follows:

$$\frac{d\Sigma_{Dif}(q)}{d\Omega} = \frac{d\Sigma_{US}(q)}{d\Omega} - \frac{d\Sigma_{C}(q)}{d\Omega}\,. \tag{10}$$

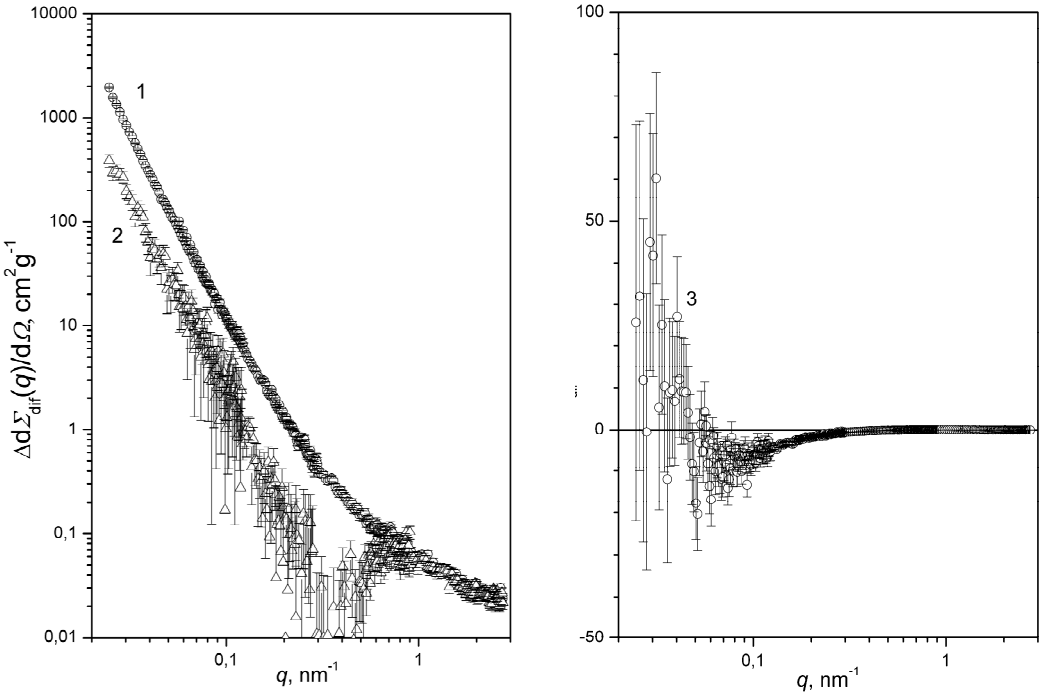

Figure 5. Differences between SANS data for sonicated and non-sonicated samples. 1, 2 and 3 – differential curves for samples obtained from 0.10, 0.25 and 1.00 mole·L^{-1} solutions, respectively.

This difference is positive over the entire q range for the xerogels prepared from 0.10 and 0.25 mole·L^{-1} solutions. This indicates that sonication results in formation of less homogeneous xerogels. For the xerogel prepared from concentrated solution (1.00 mole·L^{-1}) the opposite pattern is observed. In this case, the difference in scattering between sonicated and non-sonicated samples is positive at low and high q range only. These results are in a good agreement with the values of the integral cross-sections Σ_{tot} presented in figure 3.

Data presented in figure 4 demonstrate that surface fractal dimension of hydrated zirconia xerogels also depends upon both concentration of starting zirconium oxynitrate solution and conditions of synthesis (application of ultrasound). One can see that in general increase in concentration results in increase of surface fractal dimension. The same effect has been also observed previously for amorphous iron(III) hydroxide [5]. Probably xerogels synthesized from concentrated solutions possess

higher surface fractal dimension due to the higher frequency of colloid particles collisions during precipitation that leads to formation of more ramified structures.

Effect of ultrasonication on the surface fractal dimension of xerogels synthesized from 0.25 and 1.00 mole·L^{-1} solutions is negligible. On the other hand, application of ultrasound results in notable growth of D_S in xerogels obtained from 0.10 mole·L^{-1} solution. We believe that such an effect also originates from higher frequency of colloid particles collisions in ultrasonic field caused by microjets of liquid being formed during the collapse of cavitation bubbles.

According to XRD data thermolysis of hydrated zirconia affects phase composition and even particle size of crystalline ZrO_2 obtained through thermal treatment. Thermolysis of initial xerogels at 500 °C results in formation of tetragonal zirconia with no traces of amorphous phase or thermodynamically stable monoclinic ZrO_2. Upon the rise of the temperature up to 600 °C phase transition partially occurs and monoclinic ZrO_2 is formed. Figure 6 presents examples of X-ray diffraction patterns and the dependence of the volume fraction of tetragonal zirconia from the concentration of initial zirconium oxynitrate solution.

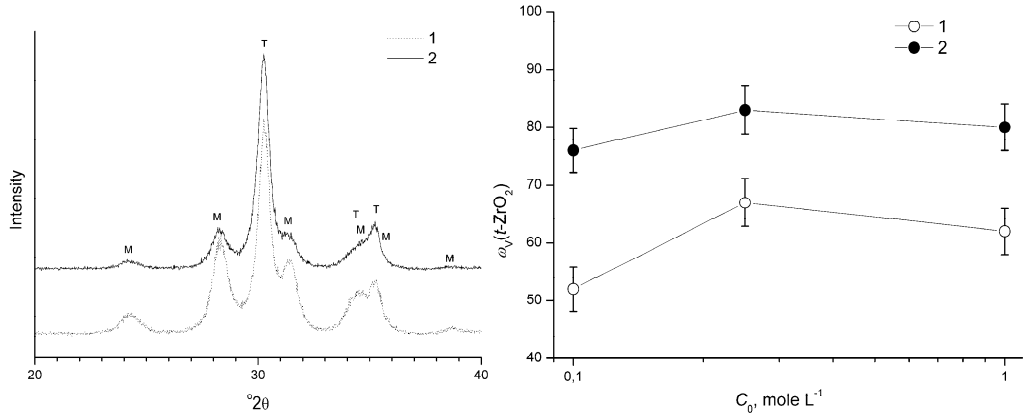

Figure 6. X-ray diffraction patterns of zirconia samples Z-1C-600 and Z-1US-600 (left) and volume fraction of tetragonal zirconia *vs*. concentration of initial solution (right). 1 – control samples; 2 – sonicated ones.

One can see that the application of ultrasound during synthesis of hydrated zirconia results in notable changes in phase composition of resulting nanocrystalline ZrO_2. Volume fraction of metastable tetragonal zirconia is higher for the samples obtained under sonication over all the concentration range.

X-ray diffraction data also demonstrate that ultrasound does not significantly affect particle size of tetragonal zirconia (see figure 7): in all the cases corresponding differences lay within the experimental error. On the other hand, increase in the concentration of starting solutions leads to a certain growth of t-ZrO_2 particle size. This effect is probably due to higher density of hydrated zirconia formed from concentrated solutions in comparison with diluted ones. Sonication of the initial gels results in slight growth of monoclinic zirconia particle size while increase in concentration of starting solution does not affect it.

Specific surface area data (see figure 7) is in a good accordance with t-ZrO_2 particle size determined from X-ray diffraction. Estimation of particle size from low-temperature nitrogen adsorption data for samples obtained from 0.10, 0.25 and 1.00 mole·L^{-1} solutions and heated at 500 °C results in the values of 15, 17 and 19–23 nm, respectively. On the other hand, one can see that thermal treatment at higher temperature (600 °C) results in notable decrease of specific surface area (S_{BET}) while particle size of t-ZrO_2 does not change significantly. This effect can not be referred to m-ZrO_2 as its particle size as estimated by Scherrer equation lies within the range of 13–17 nm for all the samples. Thus we can conclude that thermal treatment at 600 °C results in agglomeration of individual particles while this temperature is not high enough for coarsening and growth of nanocrystalline

zirconia. On the other hand these data do not confirm the supposition described elsewhere [16] dealing with stabilization of tetragonal zirconia for sub-30 nm particles of ZrO_2.

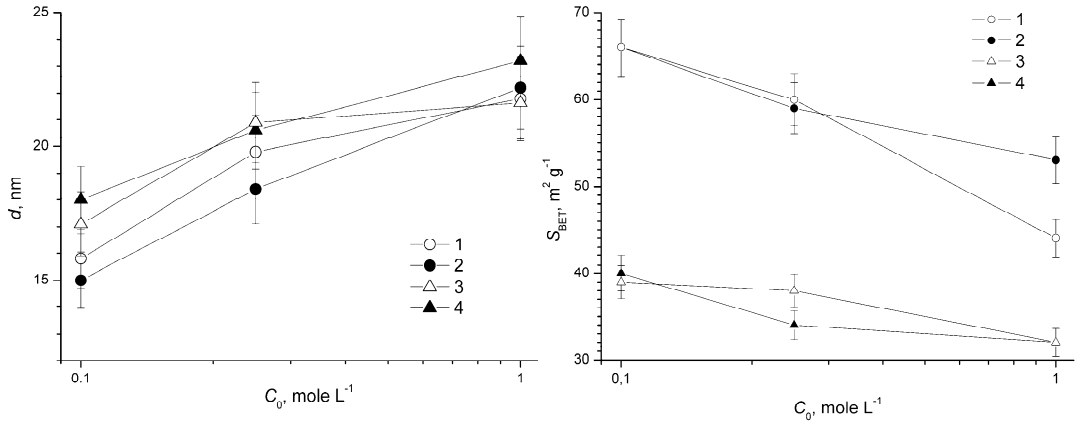

Figure 7. Particle size (left) and specific surface area (right) of tetragonal zirconia in samples heated at 500 °C (1, 2) and 600 °C (3, 4). 1,3 – control samples; 2, 4 – sonicated ones.

This work was supported by Russian Ministry of Science and Education (project 14.740.11.0281) and Russian Foundation for Basic Research (11-03-00981). G.K., A.B., S.G. and V.I. would like to thank GKSS Forschungszentrum for hearty welcome.

References

[1] Gedanken A 2004 *Ultrasonics Sonochemistry* **11** 47
Suslick K S 1999 *Ann. Rev. Matls. Sci.* **29** 295
Baranchikov A Ye, Ivanov V K and Tretyakov Yu D 2007 *Russ. Chem. Rev.* **76** 133
Meskin P E, Ivanov V K, Barantchikov A E, Churagulov B R and Tretyakov Yu D 2006 *Ultrasonics Sonochemistry* **13** 47
[2] Neppiras E A 1980 *Physics Report* **61** 159
[3] Margulis M A 2000 *Physics-Uspekhi* **43** 259
[4] Barrera-Solano M C, de la Rosa-Fox N and Esquivias L 1992 *J. Non-Cryst. Solids* **147–148** 194
Vollet D R, de Castro W C, Donatti D A and Ibañez Ruiz A 2005 *Phys. Stat. Sol.* **202** 411
Donatti D A, Vollet D R, Ibañez Ruiz A, Mesquita A and Silva T F 2005 *Phys. Rev.* B **71** 014203
[5] V.K. Ivanov, G.P. Kopitsa, F.Yu. Sharikov, A.Ye. Baranchikov, A.S. Shaporev, S.V. Grigoriev and P. Klaus Pranzas 2010 *Phys. Rev.* B **81** 174201
[6] Kopitsa G P, Ivanov V K, Grigoriev S V, Meskin P E, Polezhaeva O S and Garamus V M 2007 *JETP Letters* **85** 122
[7] Wignall G D and Bates F S 1986 *J. Appl. Cryst.* **20** 28
[8] Schmatz W, Springer T, Schelten J and Ibel K 1974 *J. Appl. Cryst.* **7** 96
[9] Gurevich I I and Tarasov T V 1965 *Physics of Low Energy Neutrons* (Moscow: Nauka) p 608
[10] Toraya H, Yoshimura M and Somiya S 1984 *J. Am. Ceram. Soc.* **67** C–119
[11] Southon P D, Bartlett J R, Woolfrey J L and Ben-Nissan B 2002 *Chem. Mater.* **14** 4313
Zyuzin D A, Moroz E M, Ivanova A S and Shmakov A N 2003 *Crystallography Reports* **48** 413
[12] Ivanov V K, Kopitsa G P, Baranchikov A E, Sharp M, Pranzas K and Grigoriev S V 2009 *Russ. J. Inorg. Chem.* **54** 2091
[13] Bale H D and Schmidt P W 1984 *Phys. Rev. Lett.* **53** 596
[14] Teixera J 1986 *On Growth and Form-Fractal and Non-Fractal Pattern in Physics* ed H E Stanley and N Ostrovsky (Boston: Martinus Nijloff) p 145
[15] Schmidt P W 1995 *Modern Aspects of Small-Angle Scattering* ed H. Brumberger (Dordrecht: Kluwer Academic Publishers) p 1

[16] Garvie R C 1965 *J. Phys. Chem.* **69** 1238
Djurado E, Bouvier P, Lucazeau G 2000 *J. Solid State Chem.* **149** 399
Shukla S, Seal S 2003 *Rev. Adv. Mater. Sci.* **5** 117